Research Square

Preprints are preliminary reports that have not undergone peer review.
They should not be considered conclusive, used to inform clinical practice,
or referenced by the media as validated information.

Intraoperative Blood Loss during Brain Arteriovenous Malformation Resection: Insights From a National Multicenter Registry

Zhinan Deng
Beijing Tiantan Hospital Affiliated to Capital Medical University
Chengzhuo Wang
Beijing Tiantan Hospital Affiliated to Capital Medical University
Heze Han
Beijing Tiantan Hospital Affiliated to Capital Medical University
Pingting Chen
Nanjing University of Aeronautics and Astronautics
Wanting Zhou
Beijing University of Posts and Telecommunications
Li Ma
University of Pittsburgh Medical Center
Haibin Zhang
Beijing Tiantan Hospital Affiliated to Capital Medical University
Qinghui Zhu
Beijing Tiantan Hospital Affiliated to Capital Medical University
Tengfei Yu
Beijing Tiantan Hospital Affiliated to Capital Medical University
Yongenbo Su
Beijing Tiantan Hospital Affiliated to Capital Medical University
Zhao Yu
Beijing Tiantan Hospital Affiliated to Capital Medical University
Yijia Chen
Beijing Tiantan Hospital Affiliated to Capital Medical University
Kexin Yuan
Peking Union Medical College Hospital
Anqi Li
Peking Union Medical College Hospital
Zhipeng Li
Peking University International Hospital
Ruinan Li

Beijing Tiantan Hospital Affiliated to Capital Medical University

Yukun Zhang
Peking University International Hospital

Hao Wang
Beijing Tiantan Hospital Affiliated to Capital Medical University

Shuo Wang
Beijing Tiantan Hospital Affiliated to Capital Medical University

Hengwei Jin
Beijing Tiantan Hospital Affiliated to Capital Medical University

Youxiang Li
Beijing Tiantan Hospital Affiliated to Capital Medical University

Dezhi Gao
Beijing Tiantan Hospital Affiliated to Capital Medical University

Shibin Sun
Beijing Tiantan Hospital Affiliated to Capital Medical University

Yuanli Zhao
Peking Union Medical College Hospital

Yu Chen
Beijing Tiantan Hospital Affiliated to Capital Medical University

Xiaolin Chen
cxl_bjtth@163.com

Beijing Tiantan Hospital Affiliated to Capital Medical University

---

Research Article

Keywords: QDSA, brain arteriovenous malformation, intraoperative blood loss

Posted Date: September 28th, 2026

DOI: https://doi.org/10.21203/rs.3.rs-10617050/v1

License: This work is licensed under a Creative Commons Attribution 4.0 International License.
Read Full License

Additional Declarations: No competing interests reported.

Abstract

Purpose

To identify the independent risk factors for major blood loss during resection of cerebral arteriovenous malformations (AVMs).

Methods

This study included 250 patients with brain AVMs who underwent microsurgical resection between January 2018 and December 2021. Patients were divided into a major intraoperative blood loss (MIBL) group (≥ 500 mL) and a non-major intraoperative blood loss (N-MIBL) group (< 500 mL). Clinical, anatomical, angioarchitectural, and quantitative digital subtraction angiography (QDSA)-derived hemodynamic parameters were collected. Univariate and multivariate logistic regression analyses were performed to identify independent factors associated with MIBL, and ROC curve analysis was used to assess the factor performance.

Results

Multivariate analysis showed that larger maximum diameter (OR = 1.03, 95% CI: 1.01–1.05, P = 0.024), presence of deep perforating artery (OR = 2.12, 95% CI: 1.12–4.02, P = 0.021), and higher D TRV (OR = 1.23, 95% CI: 1.07–1.42, P = 0.004) were independent risk factors for MIBL. In contrast, the presence of a single draining vein showed a trend to be protective (OR = 0.57, 95% CI: 0.32–1.01, P = 0.055). The optimism-corrected AUC of the multivariate model incorporating these three variables was 0.68 (95%CI: 0.64–0.71) for predicting MIBL. The optimal cutoff value for maximum diameter was 2.6 cm (sensitivity: 0.62, specificity: 0.64), and the optimal cutoff value for D TRV was 1.93 (sensitivity:0.66, specificity: 0.55).

Conclusion

Higher D TRV, along with deep perforating artery and larger maximum diameter, were associated with increased intraoperative blood loss.

Clinical Trial Registration

This study was a retrospective study using prospective national multicenter registry data from the Registry of Multimodality Treatment for Brain Arteriovenous Malformation in Mainland China (the MATCH registry, ClinicalTrials.gov register, NCT 04572568).

Introduction

Brain arteriovenous malformations (AVMs) are rare arteriovenous shunt lesions characterized by abnormal connections between cerebral arteries and veins, forming a central nidus that creates a low-resistance, high-flow structure [11]. Microsurgery is the primary treatment modality for this condition, offering advantages such as high rates of complete obliteration, immediate elimination of hemorrhagic risk, and long-term durability [14]. However, due to its highly invasive nature, microsurgery is associated with non-negligible risks. Generally, the amount of intraoperative blood loss not only reflects the surgical difficulty but also is significantly correlated with patient prognosis [33].

Factors influencing intraoperative blood loss during AVM resection remain insufficiently elucidated. Beyond the surgical technique of the operator, nidus size and Spetzler-Martin (SM) grading were considered to be potentially associated with the volume of intraoperative hemorrhage in AVM resection [16]. Nevertheless, such morphological assessments are inadequate to provide an in-depth understanding of this critical intraoperative parameter. As is well known, normal perfusion pressure breakthrough (NPPB) resulting from increased cerebral blood flow and impaired cerebral autoregulation in the perilesional brain tissue following AVM obliteration is recognized as the leading cause of postoperative hemorrhage [7, 27, 32, 24]. Therefore, the characteristic hemodynamic profile may serve as a decisive determinant of intraoperative blood loss during AVM resection. Notably, a wealth of prior studies has demonstrated that hemodynamics exerts a profound impact on AVM rupture and therapeutic prognosis [12, 23].

To address this deficiency, we incorporated the hemodynamic parameters derived from quantitative digital subtraction angiography (QDSA) into this study, including mean transit time (MTT), the Stasis Index, and transnidal relative velocity (TRV) [12, 25, 22], to provide novel insights into intraoperative blood loss during AVM resection from a hemodynamic perspective.

Methods

Study Design and Participants

This study was a retrospective study using prospective national multicenter registry data from the Registry of Multimodality Treatment for Brain Arteriovenous Malformation in Mainland China (the MATCH registry, ClinicalTrials.gov register, NCT 04572568) to investigate the quantitative hemodynamics and vascular architectural characteristics affecting the amount of blood loss during AVM resection. The MATCH registry is a nationwide multicenter prospective registry to study the natural history of AVMs in Asian population and to explore the optimal individualized treatment strategy for AVMs. Previous studies have demonstrated the database's validity and quality for research [13, 19]. The study protocol was approved by the Institutional Review Board of Beijing Tiantan Hospital (KY 2020–003 – 01). Written informed consent was obtained from all participants or their guardians at admission. This

study adhered to Helsinki Declaration guidelines and Strengthening the Reporting of Observational studies in Epidemiology (STROBE) reporting for observational case-control studies.

Patient Selection

Consecutive AVMs who underwent standalone microsurgery as initial treatment were examined between January 2018 and December 2021 from the MATCH registry. The inclusion criteria were as follows: 1) patients with AVMs received standalone microsurgery; 2) patients with preoperative original DSA images available for QDSA analysis. Exclusion criteria were as follows: 1) patients missing critical DSA images; 2) DSA data quality was suboptimal; 3) patients missing critical clinical data.

Study Parameter

We collected clinical features, anatomical structure, conventional DSA angioarchitecture, and QDSA parameters from all enrolled patients.

Clinical features included age at admission, gender, surgery type, and SM grade. Estimated blood loss was extracted from the anesthesia records. Patients with intraoperative blood loss ≥ 500 ml were defined as the major intraoperative blood loss group (MIBL). Patients with intraoperative blood loss < 500 ml were defined as the non-major intraoperative blood loss group (N-MIBL).

Anatomical structures were derived from 3T MRI, including AVM location and maximum diameter. The maximum diameter was defined as the greatest distance between two points within the nidus on the MRI plane best depicting the largest cross-sectional area.

Angioarchitectural features evaluated included feeding artery dilation, single or multiple feeding arteries, flow-related aneurysms, venous drainage type (superficial or deep), single or multiple draining veins, draining vein stenosis, venous aneurysm, and watershed AVM. The definitions for these angioarchitecture features were aligned with the guidelines established by the American Society of Interventional and Therapeutic Neuroradiology [3].

In the quantitative hemodynamic assessment, the coordinates of the time-density curve were measured using a customized program (Anythink iFlow-PLUS, Version 4.2, CREALIFE, China) for fitting (with the gamma variable function, based on the least squares method to obtain standardized time-density curves) [24]. Subsequently, we chose the lateral view of common carotid angiography images to draw ROIs. For each patient, we investigated the following ROIs: 1) cavernous sinus segment of the internal carotid (ICA); 2) distal segment of the main feeding artery; 3) AVM nidus; 4) proximal segment of the main draining vein; and 5) junction area of the draining vein and venous sinus (Fig. 1).

The calculation formulas involving the parameters were as follows: time to peak (TTP), the time required for the bolus to reach peak attenuation; mean transit time (MTT); full width at half maximum (FWHM), the duration of the time-density curve rising to 50% peak attenuation and falling to 50% peak attenuation; $ADW=\int_{T50\%A}^{T50\%v} A(t)dt$, calculated from the area under the curve (AUC) of the feeding arterial signal from Time (50% maximal arterial signal) to Time (50% maximal venous signal); transnidal relative velocity (TRV, nidus), maximum diameter (nidus)/FWHM; transvessel relative velocity (TRV, vessel), diameter (ROI)/FWHM; Stasis Index, inflow gradient/outflow gradient.

DSA Acquisition

All DSA procedures were performed with the AXIOM Artis biplane angiosuite (Artis zee, Siemens Healthineers), and a standard angiographic protocol (transfemoral route) was applied in all AVM patients. Image acquisition was performed through a 5-Fr catheter, with the tip placed at the beginning of the internal carotid artery (ICA), about 2 cm from the bifurcation of the common carotid artery. A power injector automatically injected 5 ml iodine contrast medium at a flow rate of 3 ml/sec for 1.67 seconds, and the image acquisition was achieved at a rate of 4 frames per second. The entire DSA acquisition lasted for 12 seconds, but the duration could be extended manually if necessary.

Statistical Analysis

Continuous variables were assessed for normality, and comparisons were made using the independent Student t test or Wilcoxon rank-sum test as appropriate, while categorical variables were compared using the chi-square test. Variables with a P value < .05 between two groups were selected into univariate logistic regression. Variables with a P for overall < .1 in univariate logistic regression were considered candidates for inclusion in the multivariate logistic regression model, which was constructed using stepwise regression with bidirectional elimination to identify independent factors associated with MIBL.

The predictive performance of the final multivariate model was evaluated by receiver operating characteristic (ROC) curve analysis based on the predicted probabilities. To account for overfitting, an optimism-corrected AUC was derived using the Efron–Gong bootstrap (200 resamples), and its 95% CI was obtained via the asymmetric bootstrap confidence limits for optimism-corrected measures (ABCLOC) method proposed by Frank Harrell. Additionally, ROC curve analysis was performed for individual variables to determine optimal cut-off values using the Youden index. All P values were two-sided, and statistical significance was set at P<.05.

Statistical analyses were performed using R software (version 4.5.2).

Results

Patient Selection

A total of 250 patients were included in this study, comprising 129 patients in the non-MIBL group and 121 patients in the MIBL group. Figure 2 shows the enrollment process. Baseline clinical, anatomical, angioarchitectural, and hemodynamic characteristics were compared between the two groups.

Clinical Characteristics

Patients in the MIBL group were significantly older than those in the non-MIBL group (median age: 30.44 vs. 26.20 years, P = 0.047). Ruptured AVMs was significantly fewer in the MIBL group (43.80% vs. 58.14%, P = 0.023). Notably, the MIBL group had a higher proportion of grade III (32.23% vs. 14.73%) and grade IV–V (8.26% vs. 4.65%) lesions. No significant differences were observed in gender or surgical modality (P > 0.05 for both) (Table 1).

Table 1
Clinical features between two groups

Baseline characteristics	Non-MIBL (n = 129)	MIBL (n = 121)	P value
Clinical features			
Age, M (Q_1, Q_3)	26.20 (14.70, 37.96)	30.44 (18.77, 41.81)	**0.047**
Female, n (%)	53 (41.09)	45 (37.19)	0.528
Ruptured, n (%)	75 (58.14)	53 (43.80)	**0.023**
Standalone microsurgery, n (%)			0.409
With intraoperative angiography	81 (62.79)	82 (67.77)	
SM grade, n (%)			**0.001**
I-II	104 (80.62)	72 (59.50)	
III	19 (14.73)	39 (32.23)	
IV-V	6 (4.65)	10 (8.26)	
Anatomical structure			
Maximum diameter, M (Q_1, Q_3)	2.4 (1.8, 3.3)	3.0 (2.2, 4.3)	**< .001**
Ventricular involved, n (%)	31 (24.03)	40 (33.06)	0.114
Deep location, n (%)	29 (22.48)	22 (18.18)	0.399
Infratentorial, n (%)	15 (11.63)	10 (8.26)	0.376
Angioarchitecture			
Deep venous drainage, n (%)	21 (16.28)	34 (28.10)	**0.024**
Single draining vein, n (%)	88 (68.22)	56 (46.28)	**< .001**
Drainage vein stenosis, n (%)	24 (18.60)	16 (13.22)	0.246
Venous aneurysm, n (%)	16 (12.40)	24 (19.83)	0.109
Feeding artery dilation, n (%)	59 (45.74)	69 (57.02)	0.074
Single feeding artery, n (%)	46 (35.66)	39 (32.23)	0.568
Deep perforating artery, n (%)	22 (17.05)	39 (32.23)	**0.005**
Flow-related aneurysm, n (%)	25 (19.38)	23 (19.01)	0.941
Watershed AVM, n (%)	21 (16.28)	38 (31.40)	**0.005**
Abbreviations: SM grade, Spetzler-Martin grade			

Anatomical Characteristics

The MIBL group had a significantly larger maximum diameter (median: 3.0 vs. 2.4 cm, $P < 0.001$). There were no significant between-group differences in ventricular involvement, deep location, or infratentorial location (all $P > 0.05$).

Angioarchitectural Characteristics

Several angioarchitectural features differed significantly between the two groups. The MIBL group exhibited a higher prevalence of deep venous drainage (28.10% vs. 16.28%, $P = 0.024$) and deep perforating artery feeders (32.23% vs. 17.05%, $P = 0.005$). Conversely, single draining vein was more frequently observed in the non-MIBL group (68.22% vs. 46.28%, $P < 0.001$). Additionally, watershed AVMs were more common in the MIBL group (31.40% vs. 16.28%, $P = 0.005$). No significant differences were found for other angioarchitectural features, including drainage vein stenosis, venous aneurysm, feeding artery dilation, single feeding artery, or flow-related aneurysms (all $P > 0.05$) (Table 1).

Hemodynamic Characteristics

Hemodynamic analysis revealed that the MIBL group exhibited a faster flow pattern, characterized by higher TRV (I TRV, D TRV, N TRV; all $P < 0.05$) and shorter transit times (N MTT, S TTP; both $P < 0.05$), along with reduced stasis (N Stasis Index, D Stasis Index; both $P < 0.05$). No significant differences were observed for the remaining hemodynamic parameters (all $P > 0.05$) (Table 2).

Table 2
Hemodynamics between two groups

Hemodynamics	Non-MIBL (n = 129)	MIBL (n = 121)	P value
I TTP, M (Q_1, Q_3)	1.07 (0.83, 1.50)	1.07 (1.00, 1.33)	0.719
I MTT, M (Q_1, Q_3)	1.52 (1.13, 2.29)	1.48 (1.13, 2.04)	0.315
I Stasis Index, M (Q_1, Q_3)	1.78 (1.44, 2.42)	1.74 (1.35, 2.40)	0.340
I TRV, M (Q_1, Q_3)	5.50 (3.49, 11.04)	8.06 (4.45, 12.31)	**0.017**
F TTP, M (Q_1, Q_3)	1.60 (1.25, 2.00)	1.50 (1.33, 1.87)	0.504
F MTT, M (Q_1, Q_3)	2.73 (2.30, 3.33)	2.74 (2.33, 3.14)	0.265
F Stasis Index, M (Q_1, Q_3)	2.35 (1.82, 3.06)	2.27 (1.74, 3.14)	0.734
F TRV, M (Q_1, Q_3)	1.87 (1.00, 3.25)	2.35 (1.14, 3.89)	0.110
N TTP, M (Q_1, Q_3)	2.25 (1.87, 2.75)	2.13 (1.83, 2.50)	0.101
N MTT, M (Q_1, Q_3)	3.33 (2.67, 4.03)	3.09 (2.71, 3.56)	**0.049**
N Stasis Index, M (Q_1, Q_3)	2.78 (2.23, 3.49)	2.34 (1.92, 3.27)	**0.009**
N TRV, M (Q_1, Q_3)	68.15 (31.92, 130.10)	137.10 (78.52, 217.64)	**< .001**
D TTP, M (Q_1, Q_3)	2.75 (2.25, 3.75)	2.67 (2.25, 3.17)	0.116
D MTT, M (Q_1, Q_3)	3.73 (3.03, 4.48)	3.54 (2.96, 4.15)	0.143
D Stasis Index, M (Q_1, Q_3)	2.21 (1.71, 2.92)	2.04 (1.51, 2.72)	**0.041**
D TRV, M (Q_1, Q_3)	1.76 (0.91, 3.10)	2.57 (1.48, 4.70)	**< .001**
S TTP, M (Q_1, Q_3)	3.75 (2.93, 5.50)	3.33 (2.67, 4.53)	**0.030**
S MTT, M (Q_1, Q_3)	4.53 (3.67, 5.50)	4.12 (3.60, 5.27)	0.090
S Stasis Index, M (Q_1, Q_3)	2.28 (1.79, 3.36)	2.24 (1.72, 3.17)	0.504
S TRV, M (Q_1, Q_3)	2.85 (1.72, 4.80)	3.41 (1.84, 5.09)	0.145

Abbreviations: I, internal carotid artery; F, feeding artery; N, nidus; D, draining vein; S, junction area of the draining vein and venous sinus; TTP, time to peak; MTT, mean transit time; TRV, transnidal (vessel) relative velocity

Multivariable Logistic Regression Analysis

In univariate analysis, factors with a P for overall < 0.1, including maximum diameter, single draining vein, deep perforating artery, watershed AVM, deep venous drainage, ruptured presentation, SM grade, and hemodynamic parameters (I TRV, N MTT, N TRV, D TRV, S TTP), were entered into the multivariable logistic regression model (Table 3).

Table 3
Results of univariate logistic regression

Characteristics type	OR (95%CI)	P value	P for overall
I TRV	1.03 (1.00–1.06)	0.081	**0.057**
N MTT	0.76 (0.59–0.98)	0.032	**0.024**
N Stasis Index	1.01 (0.98–1.04)	0.509	0.298
N TRV	1.005 (1.002–1.01)	< .001	**< .001**
D TRV	1.30 (1.13–1.48)	< .001	**< .001**
D Stasis Index	0.99 (0.95–1.03)	0.481	0.403
S TTP	0.90 (0.80–1.01)	0.064	**0.058**
Maximum diameter	1.04 (1.02–1.06)	< .001	**< .001**
Single draining vein	0.40 (0.24–0.67)	< .001	**< .001**
Deep perforating artery	2.31 (1.27–4.20)	0.006	**0.005**
Watershed AVM	2.35 (1.29–4.31)	0.006	**0.005**
Deep venous drainage	2.01 (1.09–3.71)	0.026	**0.024**
Age	1.01 (0.997–1.03)	0.120	0.118
Ruptured	0.56 (0.34–0.93)	0.024	**0.023**
SM grade			**0.001**
I-II	Reference	-	
III	2.96 (1.59–5.54)	< .001	
IV-V	2.41 (0.84–6.92)	0.103	

Abbreviations: I, internal carotid artery; D, draining vein; S, junction area of the draining vein and venous sinus; TTP, time to peak; MTT, mean transit time; TRV, transnidal (vessel) relative velocity; LFI, lesion-filling index; SM grade, Spetzler-Martin grade

Multivariable analysis identified three independent risk factors for MIBL: larger maximum diameter (OR = 1.03, 95% CI: 1.01–1.05, P = 0.024), presence of deep perforating artery (OR = 2.12, 95% CI: 1.12–4.02, P = 0.021), and higher D TRV (OR = 1.23, 95% CI: 1.07–1.42, P = 0.004) (Table 4). In contrast, the presence of a single draining vein showed a trend to be protective, with borderline statistical significance (OR = 0.57, 95% CI: 0.32–1.01, P = 0.055).

Table 4
Results of multivariate logistic regression

Characteristics type	OR (95%CI)	P value
D TRV	1.23 (1.07–1.42)	**0.004**
Deep perforating artery	2.12 (1.12–4.02)	**0.021**
Maximum diameter	1.03 (1.01–1.05)	**0.024**
Single draining vein	0.57 (0.32–1.01)	0.055
Abbreviations: D, draining vein; TRV, transvessel relative velocity		

Performance of the Independent Factors

Receiver operating characteristic (ROC) curve analysis was performed to evaluate the performance of the multivariable logistic regression model. After optimism correction using the Efron–Gong bootstrap method (200 resamples), the optimism-corrected area under the curve (AUC) for intraoperative blood loss was 0.68 (95% CI: 0.64–0.71) based on the model incorporating the three independent factors (maximum diameter, deep perforating artery, D TRV) (Fig. 3).

Maximum diameter and D TRV were continuous variable. For maixmum diameter (Fig. 4), the AUC was 0.65 (95% CI: 0.59–0.72). The optimal cut-off value was 2.6 cm, yielding a sensitivity of 0.62, a specificity of 0.64, and a Youden index of 0.26. For D TRV (Fig. 5), the AUC was 0.63 (95% CI: 0.57–0.70). The optimal cut-off value was 1.93, providing a sensitivity of 0.66, a specificity of 0.55, and a Youden index of 0.21.

Discussion

In this QDSA-based study, we identified larger maximum diameter, deep perforating artery feeders, and higher D TRV as independent risk factors for MIBL. D TRV showed an optimal cutoff of 1.93 (sensitivity 0.66, specificity 0.55), and maximum diameter showed an optimal cutoff of 2.6 cm (sensitivity 0.62, specificity 0.64). In the exploratory analysis, a multivariable model incorporating these three predictors demonstrated modest discriminative ability for intraoperative blood loss, with optimism-corrected AUC of 0.68 (95%CI: 0.64–0.71). This study provided clinically relevant evidence for the risk assessment of major intraoperative blood loss during brain arteriovenous malformation resection, thereby facilitating preoperative risk identification.

Massive intraoperative hemorrhage in AVM resection obscures the surgical field, prolongs operation time, induces complications, and is a key factor leading to postoperative neurological deficits, increased disability and mortality. Therefore, accurate preoperative prediction of intraoperative blood loss is clinically valuable, as it provides a basis for individualized strategies (preoperative embolization, intraoperative hemodynamic regulation, blood preparation) to reduce perioperative risks. Previous studies have confirmed that Spetzler-Martin grade, nidus size, deep venous drainage, numbers of

draining veins and high-flow are key predictors of intraoperative hemorrhage in AVM [16, 30, 10, 20]. However, current research has limitations: most focus on static angioarchitectural indicators, ignoring hemodynamic factors; and there is no precise prediction system integrating imaging, hemodynamics and clinical data to meet individualized surgical needs.

In the surgical management of AVMs, we first control and clip the lesion's feeding arteries, then dissect the surrounding brain tissue away from the malformed vascular nidus along its margins. In this step, collaborating centers of the MATCH study commonly employ a "dirty coagulation" technique for hemostasis; prior studies have demonstrated that this approach is highly effective for electrocoagulative control of perforating (penetrating) vessels around the nidus [21]. Substantial hemorrhage typically occurs during this section. In our study, large maximum diameter, higher D TRV, and deep perforating arterial supply were identified as independent predictors of MIBL. A large nidus not only implies greater surgical complexity but also greater blood volume and flow, and elevated D TRV reflects faster flow within the draining veins. A high-flow draining vein can be visualized as a tube that continuously siphons blood—the higher the flow velocity, the stronger the steal effect. Collectively, these two factors correspond to a stronger siphon (steal) effect and more pronounced blood diversion [2, 26].

The "steal" phenomenon is a characteristic feature of AVMs and can cause chronic hypoperfusion of the surrounding parenchyma, which impairs the autoregulatory capacity of perinidal vessels [4, 28]. Consequently, these vessels lose their vasodilatory responsiveness upon sudden restoration of blood flow [18]. Intraoperative interruption of the nidus redirects blood flow to the perinidal parenchyma, with several studies directly confirming increased regional perfusion during resection [5, 29, 15, 34, 9]. After shunt interruption, perinidal vessel networks are subjected to hyperperfusion, increasing intraoperative bleeding risk [31]. In addition, the proliferation of peripheral capillaries is also a typical secondary reaction caused by blood theft [4, 28]. These abnormally proliferating blood vessels are often fragile and prone to bleeding, lacking an intermediate smooth muscle layer and thus difficult to be occluded through electrocoagulation. The large maximum diameter, and the strong blood theft phenomenon indicated by high D TRV discovered in this study can provide important support for the above theory.

In addition to the above-mentioned hemodynamic mechanisms, anatomic characteristics of the AVM also substantially influence intraoperative blood loss. Deep perforating artery is closely associated with intraoperative hemorrhage because it is thin-walled, fragile, responds poorly to bipolar coagulation, and, when located in deep surgical fields, tends to retract into white matter after transection, complicating hemostasis [8, 17, 1, 6]. Besides, larger maximum diameter increases surgical complexity and the area of resection.

Accordingly, we propose that the fundamental mechanism underlying intraoperative high bleeding involves dual pathological alterations in perinidal brain tissue resulting from chronic steal, namely fragile microvasculature and impaired autoregulation. After intraoperative interruption of the nidus, abrupt flow redistribution to this vulnerable tissue, compounded by surgical trauma, triggers an NPPB-like effect.

This, together with the anatomical and technical challenges of deep perforating artery, leads to diffuse oozing and uncontrollable hemorrhage.

Limitation

This study has several limitations. First, AVM resections were performed by different attending surgeons, which may serve as an additional confounding factor affecting intraoperative blood loss. Second, quantitative digital subtraction angiography is based on two-dimensional imaging and is limited by issues such as vasculature overlap. Future hemodynamic analyses employing three- and four-dimensional imaging techniques may enable a more precise assessment of intralesional hemodynamics. Furthermore, the primary objective of this study was to explore the association between cerebral arteriovenous malformation characteristics and intraoperative blood loss, rather than to validate the predictive performance of these indicators. This limits the direct clinical applicability of our findings. To enhance the reliability and robustness of the results, a larger-sample prospective cohort study is needed to validate the conclusions of this investigation.

Conclusion

The study revealed that higher D TRV, along with deep perforating artery and larger maximum diameter, were associated with increased intraoperative blood loss.

Declarations

Acknowledgements

We sincerely express our gratitude to the research group leader Xiaolin Chen, Yu Chen, Chengzhuo Wang, Heze Han and other team members for their valuable help and support.

Author Contributions

Zhinan Deng: Conceptualization, Investigation, Methodology, Formal analysis, Writing-Original Draft; Chengzhuo Wang: Resources, Conceptualization, Investigation, Methodology, Formal analysis,; Heze Han: Invetigation, Writing-guidance; Pingting Chen and Wanting Zhou: Algorithm Support; Li Ma, Haibin Zhang, Qinghui Zhu, Tengfei Yu, Yongenbo Su, Zhao Yu, Yijia Chen, Kexin Yuan, Anqi Li, Zhipeng Li, Ruinan Li, Yukun Zhang, Hao Wang, Shuo Wang, Hengwei Jin, Youxiang Li, Dezhi Gao, Shibin Sun and Yuanli Zhao: Investigation; Yu Chen: Resources, Conceptualization, Investigation, Writing-guidance and review, Funding acquisition; Xiaolin Chen: Resources, Supervision, Funding acquisition. Zhinan Deng and Chengzhuo Wang contributed equally to this work and were considered as co-first authors. Xiaolin Chen serves as the guarantor of this study. All authors confirm that they contributed to manuscript reviews and critical revision for important intellectual content, and read and approved the final draft for submission. All authors agree to be accountable for the content of this study.

Ethical Approval and Informed Consent

All patients who enrolled in the registry gave their written informed consent at admission. The study protocol was approved by the Institutional Review Board of Beijing Tiantan Hospital (KY 2020–003-01)

Clinical Trial Registration

This study was a retrospective study using prospective national multicenter registry data from the Registry of Multimodality Treatment for Brain Arteriovenous Malformation in Mainland China (the MATCH registry, ClinicalTrials.gov register, NCT 04572568).

Conflict of Interest Disclosure

The authors declare no competing interests.

Funding Statement

Financial support and sponsor-ship: This study was supported by National Natural Science Foundation of China (Grant No. 82471302 to Xiaolin Chen; No. 82571475 to Yu Chen) and CFH-brain (Grant No. 2024-3-2051 to Yu Chen).

Data Availability

The data supporting the findings of this study are available from the corresponding author upon reasonable request. Researchers interested in accessing the data must submit a proposal detailing their research intentions to ensure alignment with ethical standards and participant confidentiality.

Permission to Reproduce Material from Other Sources

No third-party copyrighted material was used in this manuscript. All figures, tables, and other content were original creations of the authors.

Consent to Publish declaration:

The authors confirm that they have approved the final version of the manuscript and agree to its publication in BMC Surgery.

References

1. Agosti E, Graepel S, Lanzino G. Principles and strategies for step-by-step AVM excision. Neurosurg Focus. 2022;53:E5. 10.3171/2022.4.Focus21786.
2. Ansari SA, Schnell S, Carroll T, Vakil P, Hurley MC, Wu C, Carr J, Bendok BR, Batjer H, Markl M. Intracranial 4D flow MRI: toward individualized assessment of arteriovenous malformation

hemodynamics and treatment-induced changes. AJNR Am J Neuroradiol. 2013;34:1922–8. 10.3174/ajnr.A3537.

3. Atkinson RP, Awad IA, Batjer HH, Dowd CF, Furlan A, Giannotta SL, Gomez CR, Gress D, Hademenos G, Halbach V, Hemphill JC, Higashida RT, Hopkins LN, Horowitz MB, Johnston SC, Lawton MW, McDermott MW, Malek AM, Mohr JP, Qureshi AI, Riina H, Smith WS, Pile-Spellman J, Spetzler RF, Tomsick TA, Young WL. Reporting terminology for brain arteriovenous malformation clinical and radiographic features for use in clinical trials. Stroke. 2001;32:1430–42. 10.1161/01.str.32.6.1430.
4. Attia W, Tada T, Hongo K, Nagashima H, Takemae T, Tanaka Y, Kobayashi S. Microvascular pathological features of immediate perinidal parenchyma in cerebral arteriovenous malformations: giant bed capillaries. J Neurosurg. 2003;98:823–7. 10.3171/jns.2003.98.4.0823.
5. Barnett GH, Little JR, Ebrahim ZY, Jones SC, Friel HT. Cerebral circulation during arteriovenous malformation operation. Neurosurgery. 1987;20:836–42. 10.1227/00006123-198706000-00003.
6. Başkaya MK, Jea A, Heros RC. Complications of surgical treatment of arteriovenous malformations. Operative Techniques Neurosurg. 2003;6:100–4. 10.1016/s1092-440x(03)00012-4.
7. Batjer HH, Devous MD, Sr., Meyer YJ, Purdy PD, Samson DS. Cerebrovascular hemodynamics in arteriovenous malformation complicated by normal perfusion pressure breakthrough. Neurosurgery. 1988;22:503–9. 10.1227/00006123-198803000-00009.
8. Batjer HH, Devous MD, Sr., Seibert GB, Purdy PD, Bonte FJ. Intracranial arteriovenous malformation: relationship between clinical factors and surgical complications. Neurosurgery. 1989;24:75–9. 10.1227/00006123-198901000-00012.
9. Batjer HH, Purdy PD, Giller CA, Samson DS. Evidence of redistribution of cerebral blood flow during treatment for an intracranial arteriovenous malformation. Neurosurgery. 1989;25:599–604. 10.1097/00006123-198910000-00014. discussion 605.
10. Brunozzi D, Stone McGuire L, Hossa J, Atwal G, Charbel FT, Alaraj A. Preoperative embolization of brain arteriovenous malformation and efficacy in intraoperative blood loss reduction: a quantitative study. J NeuroInterventional Surg. 2024;16:541–7. 10.1136/jnis-2023-020142.
11. Chen CJ, Ding D, Derdeyn CP, Lanzino G, Friedlander RM, Southerland AM, Lawton MT, Sheehan JP. Brain arteriovenous malformations: A review of natural history, pathobiology, and interventions. Neurology. 2020;95:917–27. 10.1212/wnl.0000000000010968.
12. Chen Y, Chen P, Li R, Han H, Li Z, Ma L, Yan D, Zhang H, Lin F, Li R, Meng X, Jin H, Li Y, Ye X, Kang S, Wang H, Chen X, Zhao Y. Rupture-related quantitative hemodynamics of the supratentorial arteriovenous malformation nidus. J Neurosurg. 2023;138:740–9. 10.3171/2022.6.Jns212818.
13. Chen Y, Han H, Meng X, Jin H, Gao D, Ma L, Li R, Li Z, Yan D, Zhang H, Yuan K, Wang K, Zhang Y, Zhao Y, Jin W, Li R, Lin F, Chao X, Lin Z, Hao Q, Wang H, Ye X, Kang S, Li Y, Sun S, Liu A, Wang S, Zhao Y, Chen X. Development and Validation of a Scoring System for Hemorrhage Risk in Brain Arteriovenous Malformations. JAMA Netw Open. 2023;6:e231070. 10.1001/jamanetworkopen.2023.1070.

14. Derdeyn CP, Zipfel GJ, Albuquerque FC, Cooke DL, Feldmann E, Sheehan JP, Torner JC. Management of Brain Arteriovenous Malformations: A Scientific Statement for Healthcare Professionals From the American Heart Association/American Stroke Association. Stroke. 2017;48:e200–24. 10.1161/str.0000000000000134.
15. Dimanche A, Miller DR, Goldberg J, Raabe A, Dunn AK, Bervini D. Continuous hemodynamics monitoring during arteriovenous malformation microsurgical resection with laser speckle contrast imaging: case report. Front Surg. 2023;10. 10.3389/fsurg.2023.1285758.
16. Donzelli GF, Nelson J, McCoy D, McCulloch CE, Hetts SW, Amans MR, Dowd CF, Halbach VV, Higashida RT, Lawton MT, Kim H, Cooke DL. The effect of preoperative embolization and flow dynamics on resection of brain arteriovenous malformations. J Neurosurg. 2020;132:1836–44. 10.3171/2019.2.Jns182743.
17. Du R, Keyoung HM, Dowd CF, Young WL, Lawton MT. The Effects of Diffuseness and Deep Perforating Artery Supply on Outcomes after Microsurgical Resection of Brain Arteriovenous Malformations. Neurosurgery. 2007;60:638–48. 10.1227/01.Neu.0000255401.46151.8a.
18. Gutiérrez-González R, Pérez-Zamarron A, Rodríguez-Boto G. Normal perfusion pressure breakthrough phenomenon: experimental models. Neurosurg Rev. 2014;37:559–68. 10.1007/s10143-014-0549-3.
19. Han H, Chen Y, Ma L, Jin H, Gao D, Li Z, Li R, Zhang H, Yuan K, Li A, Yu T, Zhu Q, Wang C, Zhang Y, Zhang H, Yan D, Chao X, Lin Z, Li Y, Sun S, Zhao Y, Chen X, Wang S. Interventional Treatment vs Conservative Management of Unruptured Brain Arteriovenous Malformations. JAMA Netw Open. 2025;8:e2543408. 10.1001/jamanetworkopen.2025.43408.
20. Jafar JJ, Davis AJ, Berenstein A, Choi IS, Kupersmith MJ. The effect of embolization with N-butyl cyanoacrylate prior to surgical resection of cerebral arteriovenous malformations. J Neurosurg. 1993;78:60–9. 10.3171/jns.1993.78.1.0060.
21. Kozyrev DA, Thiarawat P, Jahromi BR, Intarakhao P, Choque-Velasquez J, Hijazy F, Teo MK, Hernesniemi J. Dirty coagulation technique as an alternative to microclips for control of bleeding from deep feeders during brain arteriovenous malformation surgery. Acta Neurochir (Wien). 2017;159:855–9. 10.1007/s00701-017-3138-8.
22. Li R, Chen P, Han H, Li Z, Chen X, Chen Y, Zhao Y. Association of nidus size and rupture in brain arteriovenous malformations: Insight from angioarchitecture and hemodynamics. Neurosurg Rev. 2023;46:216. 10.1007/s10143-023-02113-1.
23. Li R, Chen Y, Chen P, Ma L, Han H, Li Z, Zhou W, Zhou Y, Wang M, Sun S, Zhao Y, Chen X. Lesion filling index predicts brain arteriovenous malformation obliteration after Gamma knife radiosurgery: a hemodynamic analysis. Neurosurg Rev. 2024;47:889. 10.1007/s10143-024-03135-z.
24. Li Z, Chen Y, Chen P, Li R, Ma L, Yan D, Zhang H, Han H, Zhao Y, Zhang Y, Meng X, Jin H, Li Y, Chen X, Zhao Y. Quantitative evaluation of hemodynamics after partial embolization of brain arteriovenous malformations. J Neurointerv Surg. 2022;14:1112–7. 10.1136/neurintsurg-2021-018187.

25. Lin TM, Yang HC, Lee CC, Wu HM, Hu YS, Luo CB, Guo WY, Kao YH, Chung WY, Lin CJ. Stasis index from hemodynamic analysis using quantitative DSA correlates with hemorrhage of supratentorial arteriovenous malformation: a cross-sectional study. J Neurosurg. 2020;132:1574–82. 10.3171/2019.1.Jns183386.
26. Marks MP, Lane B, Steinberg G, Chang P. Vascular characteristics of intracerebral arteriovenous malformations in patients with clinical steal. AJNR Am J Neuroradiol. 1991;12:489–96.
27. Rangel-Castilla L, Spetzler RF, Nakaji P. (2015) Normal perfusion pressure breakthrough theory: a reappraisal after 35 years. Neurosurg Rev 38:399–404; discussion 404–395. 10.1007/s10143-014-0600-4
28. Sato S, Kodama N, Sasaki T, Matsumoto M, Ishikawa T. (2004) Perinidal dilated capillary networks in cerebral arteriovenous malformations. Neurosurgery 54:163–168; discussion 168–170. 10.1227/01.neu.0000097518.57741.be
29. Shellikeri S, Bai H, Setser RM, Hurst RW, Cahill AM. Association of intracranial arteriovenous malformation embolization with more rapid rate of perfusion in the peri-nidal region on color-coded quantitative digital subtraction angiography. J NeuroInterventional Surg. 2020;12:902–5. 10.1136/neurintsurg-2019-015776.
30. Shi J, Xu S, Feng Y, Wei W, Zou Y, Xiong W, Zhao W, Zhang T, Peng H, Chen J. Predicting intraoperative major blood loss in microsurgery for brain arteriovenous malformations. Front Med (Lausanne). 2024;11. 10.3389/fmed.2024.1446088.
31. Takemae T, Kobayashi S, Sugita K. (1993) Perinidal hypervascular network on immediate postoperative angiogram after removal of large arteriovenous malformations located distant from the arterial circle of Willis. Neurosurgery 33:400–405; discussion 405–406. 10.1227/00006123-199309000-00008
32. Theiss P, Alaraj A. Revisiting the normal perfusion pressure breakthrough phenomenon in the era of endovascular treatment of cerebral arteriovenous malformations. Interv Neuroradiol. 2024;15910199241254131. 10.1177/15910199241254131.
33. Wong J, Slomovic A, Ibrahim G, Radovanovic I, Tymianski M. Microsurgery for ARUBA Trial (A Randomized Trial of Unruptured Brain Arteriovenous Malformation)-Eligible Unruptured Brain Arteriovenous Malformations. Stroke. 2017;48:136–44. 10.1161/strokeaha.116.014660.
34. Ye X, Wang L, Li M-t, Chen X-l, Wang H, Ma L, Wang R, Zhang Y, Cao Y, Zhao Y-l, Zhang D, Wang S. Hemodynamic changes in superficial arteriovenous malformation surgery measured by intraoperative ICG fluorescence videoangiography with FLOW 800 software. Chin Neurosurgical J. 2020;6. 10.1186/s41016-020-00208-y.

Figures

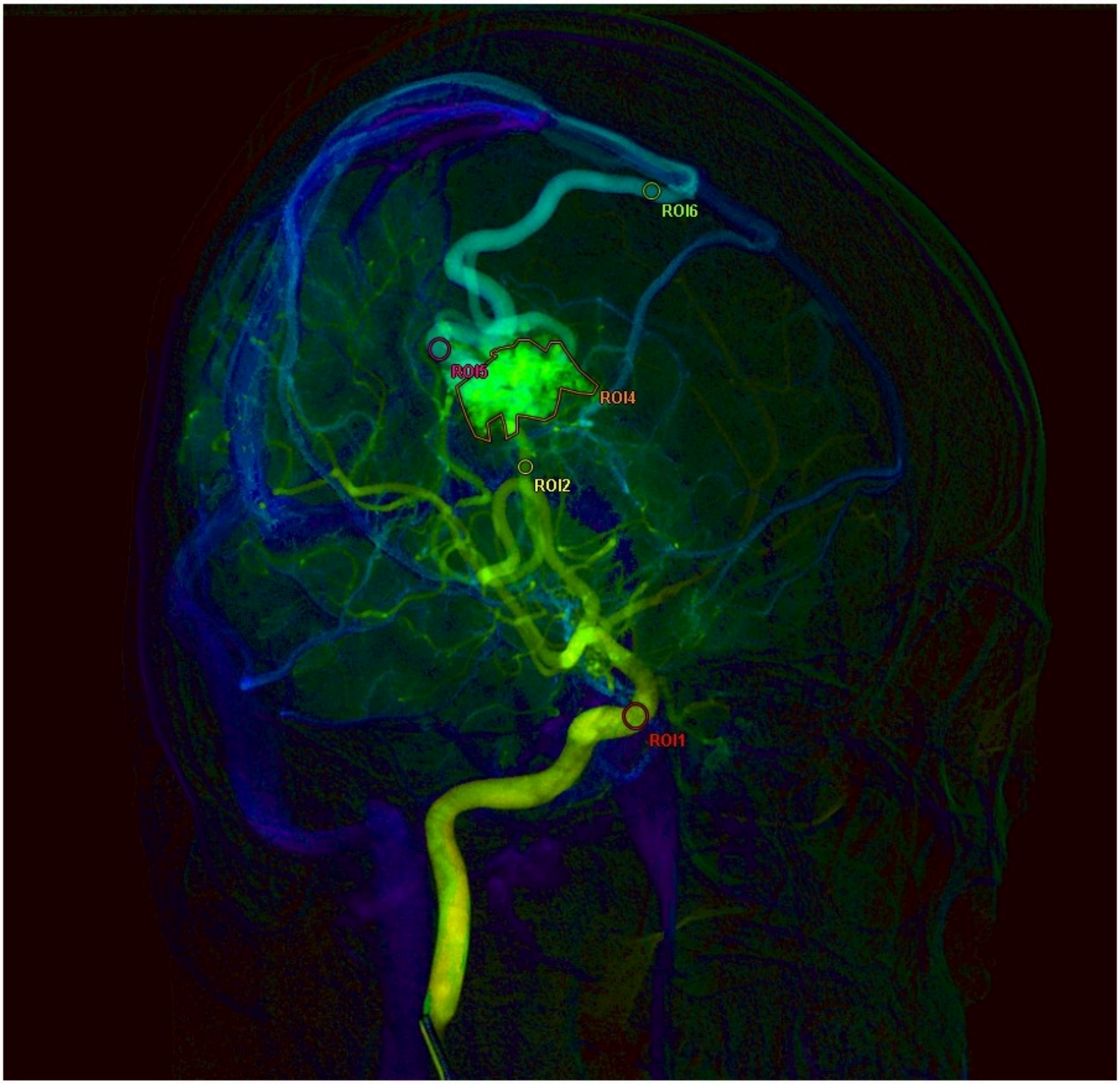


Figure 1

Legend not included with this version.

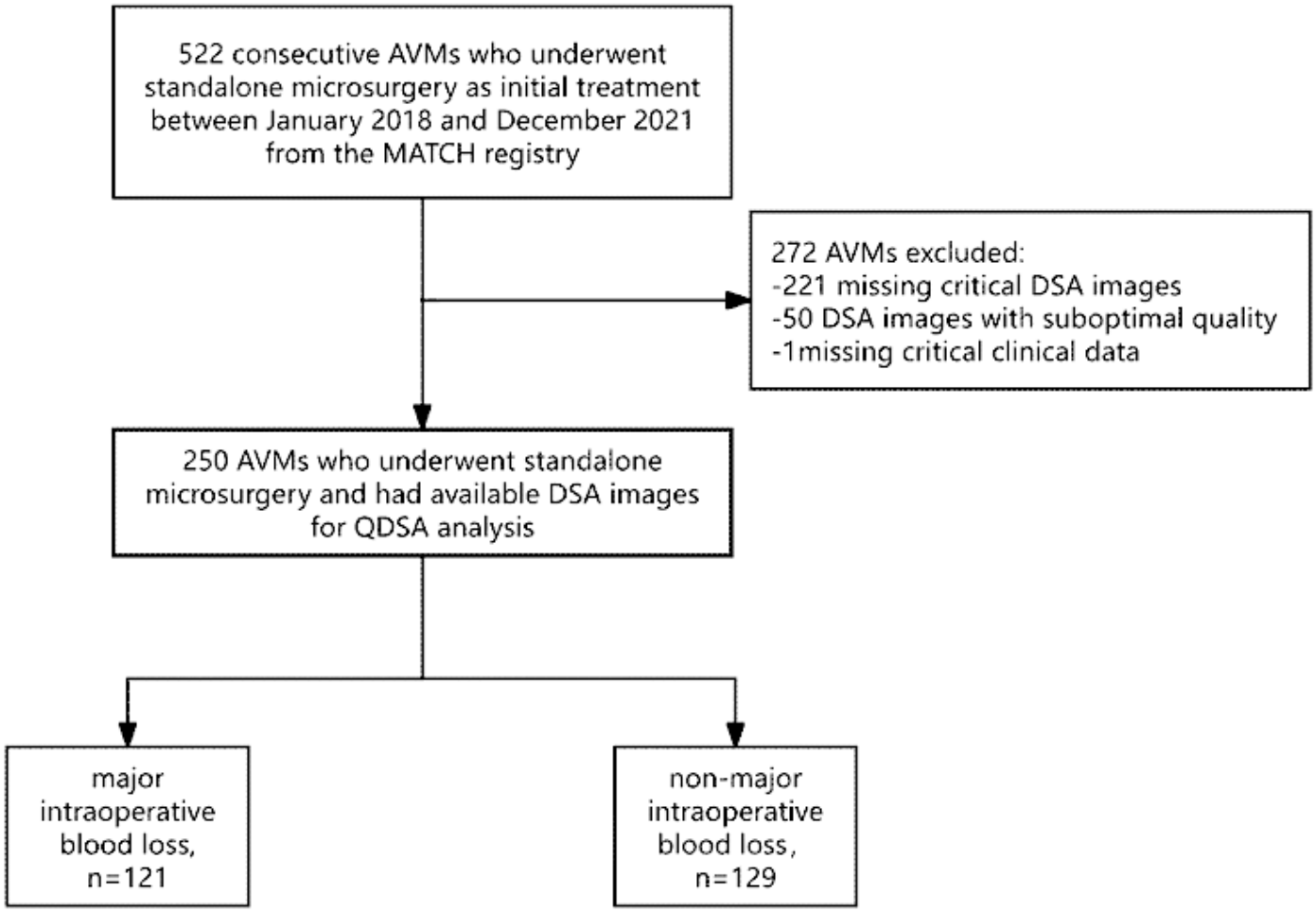


Figure 2

Legend not included with this version.

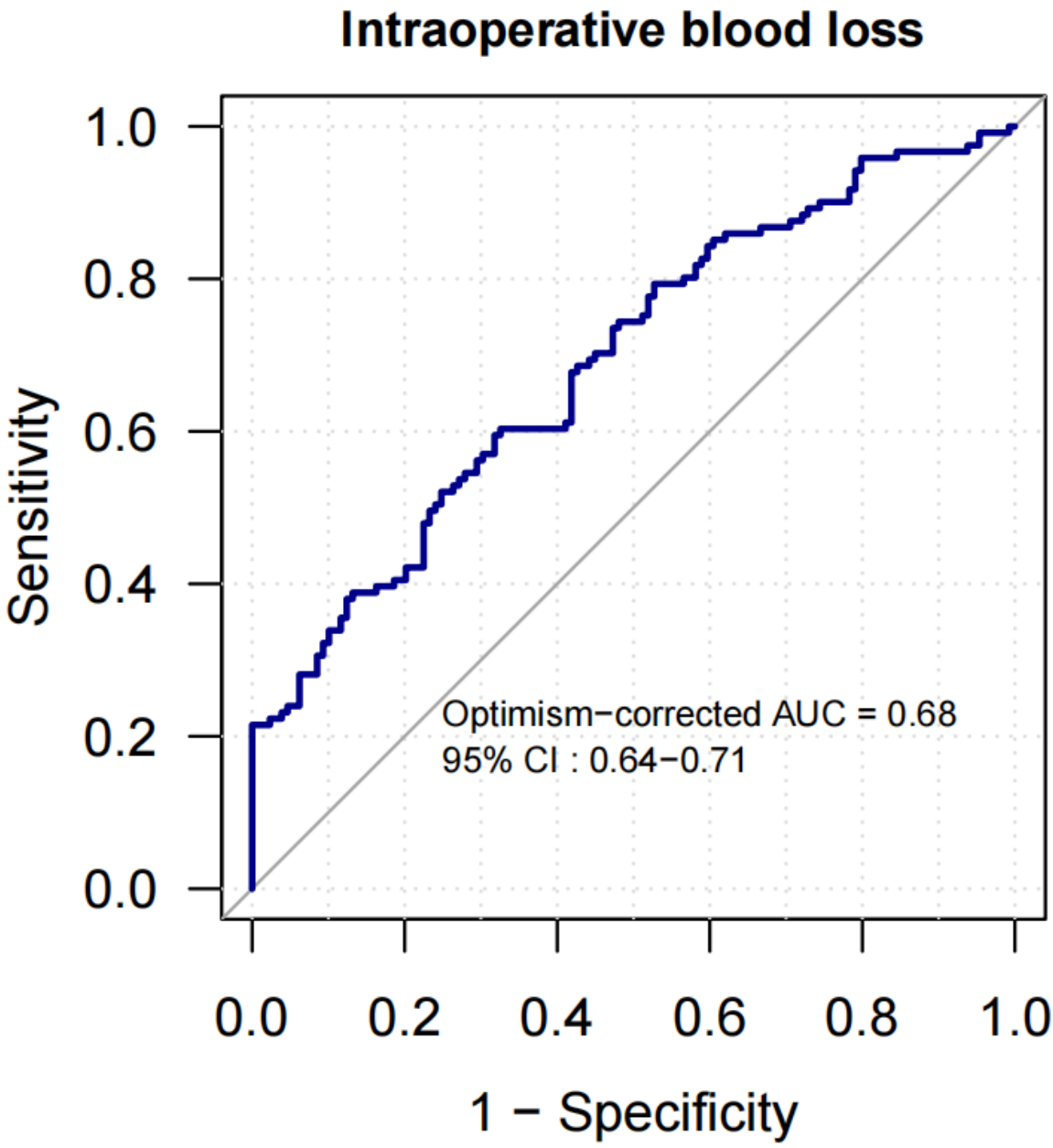


Figure 3

Legend not included with this version.

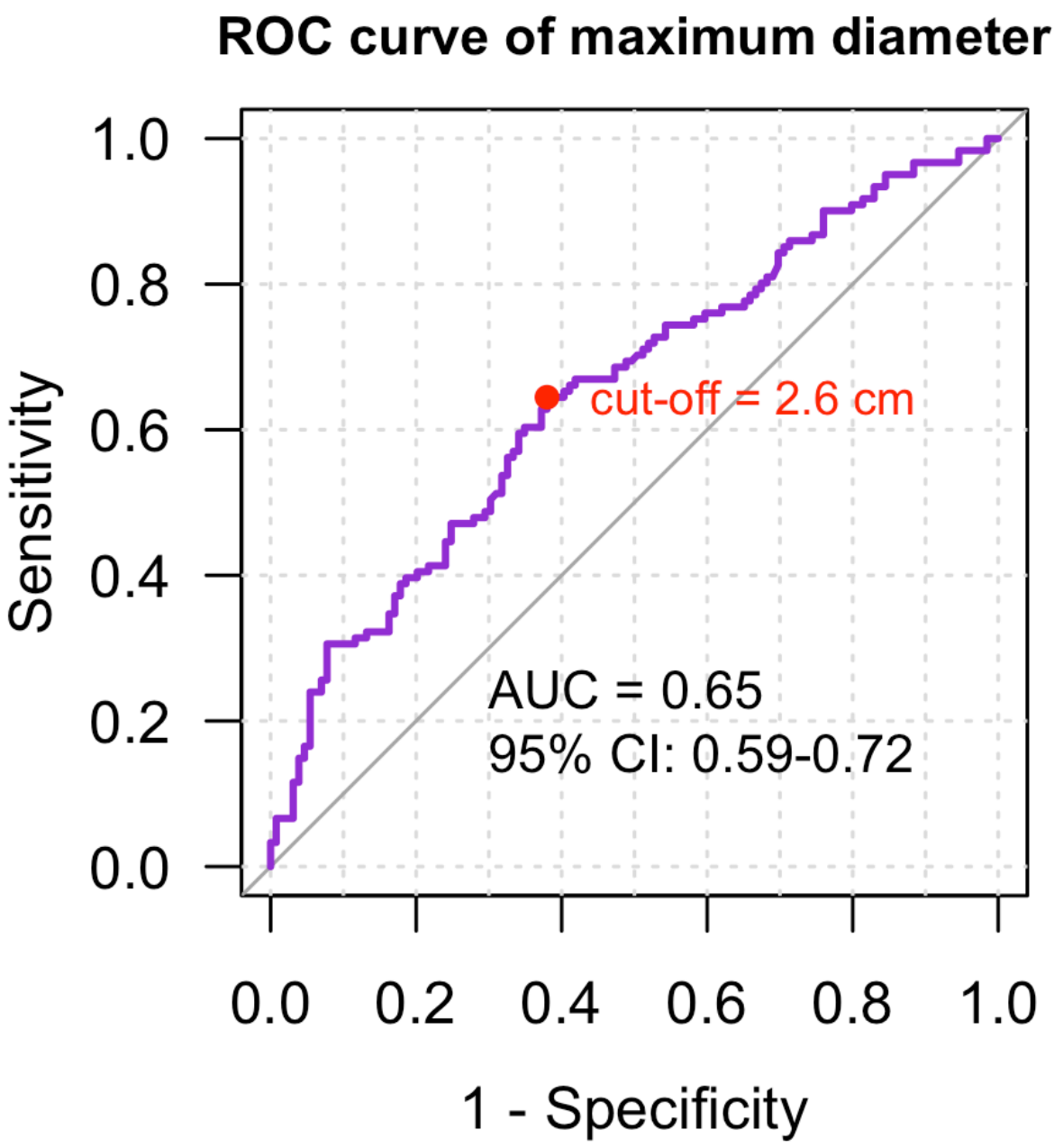


Figure 4

Legend not included with this version.

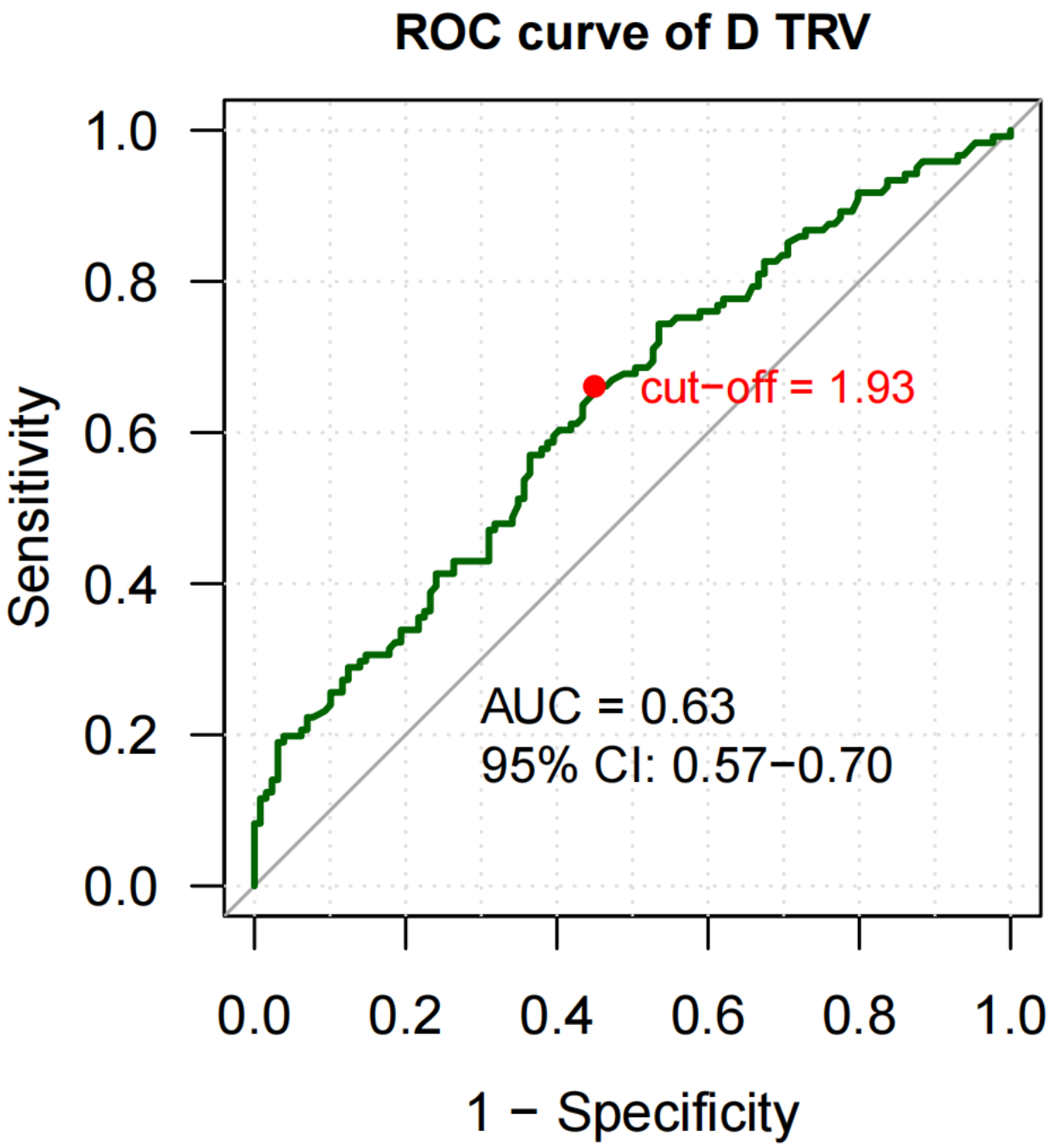


Figure 5

Legend not included with this version.